each assay of a sample. Weighing errors were minimized by using a Cahn balance and weighing 2.000-mg samples with an error of ±0.005 mg. A major problem in counting was the quenching effect of the colored products, amounting to almost 90% with **2** and 60% with **3**. Color quenching was eliminated by trifluoroacetylation, however. To do this, the 2.000-mg sample was placed in the counting vial, and 100 ± 0.1 μL of trifluoroacetic anhydride (TFA) was added. The vial was closed for 1 h at room temperature and then 10 mL of coctail (Packard SCINT-O) was pipetted into the vial. This gave a clear, colorless solution for counting. Trial experiments with standard samples and with **2** and **3** showed that this way of using TFA gave reasonably reproducibly results. Our overall practice then was to assay each of three separate 2.000-mg samples of each product according to the restrictions given above. An assay was made by making 10 timed, programmed counts, each count being of the order of 225 000. The 10 counts were then averaged, and the assays gave, eventually, three averaged counts for each sample of **2** and **3** at 30% and three averaged counts at 100% conversion. The deviation among the three averaged counts of samples at 30% conversion was often somewhat greater than the deviation among the three averaged counts at 100% conversion. Thus, the average of errors among all of the 30% conversion counts for **2** and **3** amounted to 0.22% while the average of errors among the 100% conversion counts was 0.15%. Four separate runs were made with [2-^{14}C]-**1** (one in the presence of HQ), and two were made with [4-^{14}C]-**1**. The calculated KIE are listed in Table II.

The data in Tables I and II list average errors in KIE. Calculations of the nitrogen KIE involve the terms $[(M + 1)/M]_{low}$ and $[(M + 1)/M]_{100}$ where low refers to 20% or 30% conversions and 100 refers to 100% conversion. The standard deviations in abundance measurements were used, therefore, to calculate a maximum and minimum measurement of an enriched (M + 1) abundance, normalized against 100% abundance for M and corrected for the natural abundance of (M + 1). Thus, for each conversion, low and 100%, we had, eventually, a maximum and minimum measure of the enrichment, mass (M + 1). Maximum and minimum KIE were calculated from these data for each run and expressed as an average in Table I. Calculations of carbon KIE also reflect the standard deviation in the average of three assays per sample. Thus, a maximum and minimum count was obtained for each sample at each conversion, and these led to a maximum and minimum KIE in each run, the average of which is expressed in Table II.

Registry No. [$^{15}NO_2$]-**1**, 90047-95-3; [2-^{14}C]-**1**, 90047-96-4; [4-^{14}C]-**1**, 90047-97-5; carbon-14, 14762-75-5; nitrogen-15, 14390-96-6.

Characterization of Molecular Aggregates of Peptide Amphiphiles and Kinetics of Dynamic Processes Performed by Single-Walled Vesicles

Yukito Murakami,* Akio Nakano, Akira Yoshimatsu, Kunio Uchitomi, and Yoshihisa Matsuda

Contribution No. 712 from the Department of Organic Synthesis, Faculty of Engineering, Kyushu University, Fukuoka 812, Japan. *Received June 30, 1983*

Abstract: Peptide amphiphiles involving an L-alanine residue interposed between a charged head group and a double-chain segment, $N^+C_mAla2C_n$, were prepared, and the morphology of their aggregates in aqueous media was investigated by electron microscopy. Differential scanning calorimetry (DSC) was applied to examine thermodynamic properties of the bilayer aggregates associated with the phase transition between the gel and liquid-crystalline states. Appropriate lengths of the molecular skeleton ($n + m \leq 21$) and the double-chain segment ($12 \leq n \leq 16$) are required to obtain stable single-walled vesicles having the internal aqueous compartment under moderate sonication conditions. The exchange of amphiphile molecules between single-walled bilayer vesicles of a peptide amphiphile ($N^+C_5Ala2C_{16}$) and those of the corresponding spin-labeled amphiphile (SP-$N^+C_5Ala2C_{16}$) was investigated in a phosphate–borate buffer (pH 6.70, μ 0.10 with KCl) at 10.0–35.0 °C. The exchange took place via a collision mechanism rather than a diffusion-mediated process. The flip–flop behavior of the amphiphile molecules in the bilayer membrane, the permeability of sodium ascorbate into the vesicle, and the leakage of a water-soluble spin probe from the internal aqueous compartment of the vesicle were examined in the same medium. The single-walled vesicles thus prepared are stable enough to inhibit fusion under ordinary conditions.

Currently, there is growing interest in the physical properties and aggregation behavior of naturally occurring[1] and synthetic bilayer membranes.[2] Although the structures of phospholipid bilayers have been extensively investigated in connection with their biological functions,[3] their complexities and chemical instabilities have necessitated the development of more stable membrane-forming amphiphiles. Much effort has recently been exerted along this line, and a large number of membrane-forming amphiphiles have been prepared.[2] On the basis of electron microscopy, previous workers have claimed success in preparing several amphiphiles that form single-walled vesicles, having the internal aqueous compartment, without adding secondary components.[2a,j,4] We have recently shown that amphiphiles involving amino acid residues of various nature interposed between a polar head moiety and an aliphatic double-chain segment form distinct single-compartment vesicles in aqueous media, and such vesicles retain the morphology for a reasonably prolonged period of time.[5] In the light of the

(1) (a) Bangham, A. D.; Standish, M. M.; Watkins, J. C. *J. Mol. Biol.* **1965**, *13*, 238–252. (b) Huang, C. *Biochemistry* **1969**, *8*, 344–351.

(2) (a) Kunitake, T.; Okahata, Y.; Shimomura, M. Yasunami, S.; Takarabe, K. *J. Am. Chem. Soc.* **1981**, *103*, 5401–5413 and references therein. (b) Tundo, P.; Kippenberger, D. J.; Klahn, P. L.; Prieto, N. E.; Jao, T.-C.; Fendler, J. H. *Ibid.* **1982**, *104*, 456–461. (c) Deguchi, K.; Mino, J. *J. Colloid Interface Sci.* **1978**, *65*, 155–161. (d) Mortara, R. A.; Quina, F. H.; Chaimovich, H. *Biochem. Biophys. Res. Commun.* **1978**, *81*, 1080–1086. (e) Czarniecki, M. F.; Breslow, R. *J. Am. Chem. Soc.* **1979**, *101*, 3675–3676. (f) Sudhölter, E. J. R.; de Grip, W. J.; Engberts, J. B. F. N. *Ibid.* **1982**, *104*, 1069–1072. (g) Regen, S. L.; Singh, A.; Oehme, G.; Singh, M. *Ibid.* **1982**, *104*, 791–795. (h) Baumgartner, E.; Fuhrhop, J.-H. *Angew. Chem., Int. Ed. Engl.* **1980**, *19*, 550–551. (i) Moss, R. A.; Bizzigotti, G. O. *J. Am. Chem. Soc.* **1981**, *103*, 6512–6514. (j) Lopez, E.; O'Brien, D. F.; Whitesides, T. H. *Ibid.* **1982**, *104*, 305–307. (k) Akimoto, A.; Dorn, K.; Gros, L.; Ringsdorf, H.; Schupp, H. *Angew. Chem., Int. Ed. Engl.* **1981**, *20*, 90–91.

(3) (a) Ansell, G. B.; Dauson, R. M. C.; Hawthorne, J. N., Eds. "Form and Function of Phospholipids"; Elsevier: Amsterdam, 1973. (b) Jain, M. K.; Wagner, R. C. "Introduction to Biological Membranes"; Wiley: New York, 1980. (c) Chapman, D., Ed. "Biological Membranes"; Academic Press: New York, 1968.

(4) Kunitake, T.; Nakashima, N.; Shimomura, M.; Okahata, Y.; Kano, K.; Ogawa, T. *J. Am. Chem. Soc.* **1980**, *102*, 6642–6644.

0002-7863/84/1506-3613$01.50/0

Table I. Physical and Analytical Data of Amphiphiles

amphiphile	formula	elemental analysis,[a] % C	H	N	mp,[b] °C	$[\alpha]^{20}_D$,[c] deg
$N^+C_5Ala2C_8$	$C_{28}H_{58}N_3O_2Br + H_2O$	59.59 (59.34)	10.61 (10.67)	7.31 (7.41)	120	−18.2 (1.21)
$N^+C_5Ala2C_{10}$	$C_{32}H_{66}N_3O_2Br$	63.38 (63.55)	10.91 (11.00)	6.61 (6.95)	142	−23.5 (1.01)
$N^+C_5Ala2C_{12}$	$C_{36}H_{74}N_3O_2Br$	65.07 (65.42)	11.27 (11.28)	6.09 (6.36)	195	−18.5 (0.91)
$N^+C_5Ala2C_{14}$	$C_{40}H_{82}N_3O_2Br + {}^1/_2H_2O$	66.24 (66.17)	11.45 (11.52)	5.77 (5.78)	225	−15.5 (1.03)
$H^+C_5Ala2C_{16}$	$C_{44}H_{90}N_3O_2Br + {}^1/_2H_2O$	67.60 (65.57)	11.68 (11.73)	5.35 (5.37)	226	−18.0 (1.11)
$N^+C_5Ala2C_{18}$	$C_{48}H_{98}N_3O_2Br + H_2O$	68.20 (68.05)	11.81 (11.90)	4.87 (4.96)	208	−14.2 (1.13)
$N^+C_2Ala2C_{16}$	$C_{41}H_{84}N_3O_2Br + H_2O$	65.69 (65.74)	11.31 (11.57)	5.64 (5.61)	200	−10.6 (1.04)
$N^+C_7Ala2C_{16}$	$C_{46}H_{94}N_3O_2Br + H_2O$	67.92 (67.45)	11.70 (11.81)	5.22 (5.13)	222	−18.4 (1.14)
$N^+C_{10}Ala2C_{16}$	$C_{49}H_{100}N_3O_2Br + {}^1/_2H_2O$	69.38 (69.06)	11.89 (11.94)	5.01 (4.93)	187	−18.9 (1.17)

[a] Calculated values are given in parentheses. [b] Final melting point to liquid state. [c] Amphiphile concentration in ethanol (g/100 mL) is given in parentheses.

tripartite structure concept for biomembranes,[6] we claimed that a hydrogen-belt domain is constructed through intermolecular hydrogen-bonding interaction between amino acid residues in each vesicle. Such intravesicular interaction may act to tighten the aggregate structure as confirmed by various physicochemical methods.[5] In the present work, we have clarified the threshold range for bilayer vesicle formation with respect to their aliphatic double-chain length. The L-alanine residue was used exclusively as an amino acid component that may constitute a hydrogen-belt domain upon formation of vesicles. The thermodynamic properties of the present vesicles associated with the phase transition between the gel and liquid-crystalline states and their chemical stabilities have been discussed in comparison with those of phospholipid liposomes.

The exchange of lipid molecules between membranes is an important dynamic event in biological systems. The study of interaction between artificial model membranes represents a simplified approach to the basic problem of membrane–membrane interactions and has shed some light on the nature of intermembrane amphiphile exchange.[7] The latter has been suggested to occur either by lipid transfer as monomers or micelles through the bulk aqueous phase[7,8] or by lipid transfer upon collision of the membranes.[9] The molecular mechanism of biological membrane fusion has received a great deal of attention since this process plays an important role in biological functions such as storage, reproduction, simulation, and response. Application of these artificial vesicle systems, which serve as simplified models for biological membranes, also provides a means of clarifying structural parameters for cell–cell and vesicle–cell fusions that occur in natural systems.[10] Other purposes of the present study are to clarify the dynamic behavior of spontaneous exchange of the peptide amphiphile molecules between their vesicles and to examine the possibility of fusion process of their single-walled vesicles by the ESR technique. The exchange process of the spin-labeled amphiphile molecules (SP-$N^+C_5Ala2C_{16}$) with the unlabeled ones ($N^+C_5Ala2C_{16}$) in their respective vesicular states and the fusion of vesicles of the latter amphiphile, which contain a water-soluble spin probe (SP) and a reducing agent separately in their inner water pool, have been directly assayed by the ESR method.

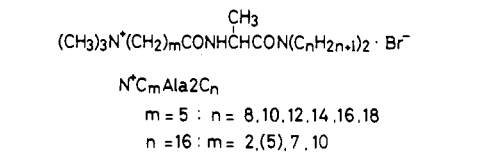

$N^+C_mAla2C_n$

m = 5 : n = 8,10,12,14,16,18

n = 16 : m = 2,(5),7,10

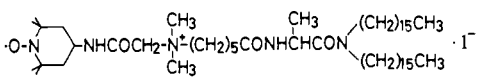

SP-$N^+C_5Ala2C_{16}$

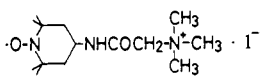

SP

Experimental Section

Materials. Dimyristoyl-L-α-phosphatidylcholine (DMPC) was purchased from Sigma Chemical Co. (purity 98%) and used without further purification. Sodium L-ascorbate (Asc^-), myristic acid, myristylamine, and citric acid of extra pure grade were obtained from Wako Pure Chemical Industries, Osaka, Japan. Cholesterol of extra pure grade was purchased from Ishizu Pharmaceutical Co., Osaka, Japan, and used without further purification. Peptide amphiphiles having the L-alanine residue ($N^+C_mAla2C_n$) were prepared according to the procedure similar to that used for the synthesis of $N^+C_5Ala2C_{12}$.[5d] The physical and analytical data for the present amphiphiles are summarized in Table I. The NMR and IR spectral data for the amphiphiles are almost identical with those reported previously for $N^+C_5Ala2C_{12}$.[5d] The spin-labeled amphiphile, SP-$N^+C_5Ala2C_{16}$, was synthesized from *N*-(1-oxyl-2,2,6,6-tetramethyl-4-piperidyl)iodoacetamide and *N*,*N*-dihexadecyl-N^α-[6-(dimethylamino)hexanoyl]-L-alaninamide ($2C_1NC_5Ala2C_{16}$). The former compound (spin-labeled segment) was prepared according to the procedure reported by McConnell et al.[11]

***N*,*N*-Dihexadecyl-N^α-[6-(dimethylamino)hexanoyl]-L-alaninamide ($2C_1NC_5Ala2C_{16}$).** This material was prepared by a procedure similar to that reported for the synthesis of *N*,*N*-didodecyl-N^α-[6-(dimethylamino)hexanoyl]-L-alaninamide:[5d] white glassy solid, final mp 38.0–40.0 °C; IR (neat) ν_{max} 3240 (NH), 2880 and 2820 (CH), 1640 (C=O) cm^{-1}; ^1H NMR ($CDCl_3$, Me_4Si) δ 0.87 [6 H, br t, $(CH_2)_{15}CH_3$], 1.00–2.00 [6 H, m. $NCH_2(CH_2)_3CH_2CO$], 1.26 [59 H, s, $CH_2(CH_2)_{14}CH_3$ and $CH(CH_3)CO$], 2.18 [6 H, s, $(CH_3)_2N$], 2.22 [2 H, t, $N(CH_2)_4CH_2CO$], 3.23 [6 H, br t, $(CH_3)_2NCH_2(CH_2)_4$ and $NCH_2(CH_2)_{14}CH_3$], 4.85 [1 H, br q, $CH(CH_3)CO$], 6.50 [1 H, d, $CONHCH(CH_3)$].

***N*,*N*-Dihexadecyl-N^α-[6-[*N*-[(((1-oxyl-2,2,6,6-tetramethyl-4-piperidyl)carbamoyl)methyl)dimethylammonio]hexanoyl]-L-alaninamide Iodide (SP-$N^+C_5Ala2C_{16}$).** $2C_1NC_5Ala2C_{16}$ (610 mg, 0.9 mmol) and *N*-(1-oxyl-2,2,6,6-tetramethyl-4-piperidyl)iodoacetamide (608 mg, 1.8 mmol) were dissolved in dry methanol (3 mL), and the mixture was stirred for 6 days at 20–25 °C. The reaction mixture was then subjected to gel-filtration chromatography (Sephadex LH-20, methanol as an

(5) (a) Murakami, Y.; Nakano, A.; Fukuya, K. *J. Am. Chem. Soc.* **1980**, *102*, 4253–4254. (b) Murakami, Y.; Nakano, A.; Yoshimatsu, A.; Fukuya, K. *Ibid.* **1981**, *103*, 728–730. (c) Murakami, Y.; Aoyama, Y.; Nakano, A.; Tada, T.; Fukuya, K. *Ibid.* **1981**, *103*, 3951–3953. (d) Murakami, Y.; Nakano, A.; Ikeda, H. *J. Org. Chem.* **1982**, *47*, 2137–2144. (e) Murakami, Y.; Aoyama, Y.; Kikuchi, J.; Nishida, K.; Nakano, A. *J. Am. Chem. Soc.* **1982**, *104*, 2937–2940. (f) Murakami, Y.; Nakano, A.; Akiyoshi, K. *Bull. Chem. Soc. Jpn.* **1982**, *55*, 3004–3012.

(6) Brockerhoff, H. In "Bioorganic Chemistry"; van Tamelen, E. E., Ed.; Academic Press: New York, 1977; Vol. 3, Chapter 1.

(7) Martin, F. J.; MacDonald, R. C. *Biochemistry* **1976**, *15*, 321–327.

(8) (a) Roseman, M. A.; Thompson, T. E. *Biochemistry* **1980**, *19*, 439–444. (b) Papahadjopoulos, D.; Hui, S.; Vail, W. J.; Poste, G. *Biochim. Biophys. Acta* **1976**, *448*, 245–264. (c) Duckwitz-Peterlein, G.; Eilenberger, G.; Overath, P. *Ibid.* **1977**, *469*, 311–325. (d) Nichols, J. W.; Pagano, R. E. *Biochemistry* **1981**, *20*, 2783–2789. (e) De Cuyper, M.; Joniau, M.; Dangreau, H. *Biochem. Biophys. Res. Commun.* **1980**, *95*, 1224–1230.

(9) (a) Kremer, J. M. H.; Kops-Werkhoven, M. M.; Pathmamanoharan, C.; Gijzeman, O. L. J.; Wiersema, P. H. *Biochim. Biophys. Acta* **1977**, *471*, 177–188. (b) Maeda, T.; Ohnishi, S. *Biochem. Biophys. Res. Commun.* **1974**, *60*, 1509–1516.

(10) Prestegard, J. H.; Fellmeth, B. *Biochemistry* **1974**, *13*, 1122–1126.

(11) McConnell, H. M.; Deal, W.; Ogata, R. T. *Biochemistry* **1969**, *8*, 2580–2585.

Table II. Initial Concentrations of Various Species for Studies of Dynamic Processes[a]

process entity	$N^+C_5Ala2C_{16}$, mM	SP-$N^+C_5Ala2C_{16}$, mM	SP, mM	Asc^-, mM
amphiphile exchange	7.10–24.3	0.25		
	18.5	0.13–0.37		
amphiphile flip–flop	19.6	0.39		
permeation of Asc^-	9.8	0.19		49.0 (bulk)[b]
leakage of SP	9.8		4.94 (vesicle)[c]	49.0 (bulk)[d]
vesicular fusion	9.8		4.94 (A vesicle)[c]	98.0 (B vesicle)[c]
				49.0 (bulk)[d]

[a] All the measurements were carried out in KH_2PO_4 (69 mM)–$Na_2B_4O_7$ (15 mM) aqueous buffer at pH 6.70 and μ 0.1 (KCl); temperature was maintained constant during each run. [b] Concentration in bulk aqueous phase. [c] Concentration in the internal aqueous compartment of vesicle. [d] Concentration in bulk aqueous phase before quenching SP initially present in bulk aqueous phase.

eluant). A pale yellow fraction eluted first was collected and evaporated to dryness. The residual dark red liquid was purified further by liquid chromatography on a column of silica gel (Wako gel C-100). The column was first washed with chloroform to remove a trace amount of the excess starting material and then eluted with chloroform–methanol (3:1 v/v). Elimination of the solvent in vacuo under nitrogen gave a viscous oil of dark red color: yield 850 mg (93%); IR (neat) ν_{max} 3270 (NH), 2920 and 2850 (CH), 1675 and 1635 (C=O) cm^{-1}. Anal. Calcd for $C_{54}H_{107}N_5O_4I$: C, 63.75; H, 10.60; N, 6.88. Found: C, 63.53, H, 10.56; N, 6.80.

***N*-[((1-Oxyl-2,2,6,6-tetramethyl-4-piperidyl)carbamoyl)methyl]trimethylammonium Iodide (SP).** Dry trimethylamine gas was introduced into a dry benzene solution (20 mL) of *N*-(1-oxyl-2,2,6,6-tetramethyl-4-piperidyl)iodoacetamide (300 mg, 0.9 mmol) over a period of 2 h at room temperature, and the solution was stirred overnight at the same temperature. After benzene was removed in vacuo, the residue was recrystallized from ethanol: yield 310 mg (88%); mp 235–238 °C dec; IR (KBr disk) ν_{max} 3270 (NH), 2960 and 2920 (CH), 1670 (C=O) cm^{-1}. Anal. Calcd for $C_{14}H_{29}N_3O_2I$: C, 42.21; H, 7.33; N, 10.54. Found: C, 42.20; H, 7.30; N, 10.37.

General Measurements. IR spectra were taken on a JASCO DS-403G grating spectrophotometer. NMR spectra were obtained with a Hitachi Perkin-Elmer R-20 spectrometer; tetramethylsilane in deuteriochloroform and 3-(trimethylsilyl)propanesulfonic acid in deuterium oxide were used as internal references. Melting points were measured on a Yanaco MP-S1 melting point apparatus (hot-plate type) with a filter for polarized light. Optical rotations were measured with a Union Giken PM-71 high-sensitivity polarimeter. ESR spectra were recorded on a JEOL JES-ME-3 X-band spectrometer equipped with a 100-kHz field modulation unit; a standard MgO/Mn^{II} sample calibrated with a NMR magnetometer was used for calibration of the magnetic field.

Electron Microscopy. Aqueous dispersions (A) and ultrasonicated aqueous solutions (B) of amphiphiles were employed. The samples were prepared by the following procedure unless otherwise stated. For sample A, 6–9 mg of an amphiphile was suspended in 2 mL of deionized and distilled water containing 2 w/w % uranyl acetate, and the dispersion was shaked occasionally and heated until the glassy solid disappeared completely to give a turbid dispersion. For sample B, an aqueous dispersion of an amphiphile (sample A) was sonicated for 2 min with a probe-type sonicator at 30 W (W-220F, Heat Systems-Ultrasonics) and allowed to stand for 10 min at 5 °C. A clear solution was then obtained. Samples A and B were applied on carbon grids and dried in a vacuum desiccator. A JEOL JEM-200B electron microscope, installed at the Research Laboratory for High Voltage Electron Microscopy of Kyushu University, was used for the measurements.

Differential Scanning Calorimetry (DSC). The phase transition temperature (T_m, temperature at a peak maximum of DSC thermogram) for an amphiphile was measured with a differential scanning calorimeter (Daini Seikosha SSC-560U): heating rate, 2 °C/min; chart speed, 0.5 cm/min; sensitivity, 0.025 (mcal/s)/(full scale); temperature and transition heat being calibrated with benzophenone (48 °C) and/or water (0 °C). Each 50-μL sample of an aqueous dispersion [ca. 2.0 w/w %, 0.023–0.033 M] in redistilled and deionized water was weighed and sealed into a silver capsule. As for amphiphiles that have T_m's close to 0 °C, the sample was supercooled to ca. −10 °C without freezing of water, and then the temperature was raised gradually at 1 °C/min. The enthalpy change for phase transition (ΔH) was determined by measuring the peak area of the DSC thermogram. The accuracy ranges for T_m and ΔH were within ±0.5 °C and ±10%, respectively.

Amphiphile Exchange Measurements. An aqueous suspension of an appropriate amount of $N^+C_5Ala2C_{16}$ in a phosphate–borate buffer (69 mM KH_2PO_4 and 15 mM $Na_2B_4O_7$: 2 mL; pH 6.70, μ 0.1 with KCl) was sonicated for 5 min with a probe-type sonicator (Heat Systems-Ultrasonics, Model W-220F) to obtain a clear solution. A vesicle solution of SP-$N^+C_5Ala2C_{16}$ was prepared by the similar procedure in a relatively short sonication period (1 min) to avoid degradation of the amphiphile, which may occur under prolonged sonication conditions. Each aliquot (1 mL) was pipeted out from the above sonicated solutions kept at 0 °C, and these samples were mixed together at the same temperature. A 50-μL sample of the mixture was transferred to an ESR cell by using a microsyringe for the measurements.

Vesicular Fusion Measurements. A mixture of an appropriate amount of $N^+C_5Ala2C_{16}$ and 4.94 mM SP (or 98.0 mM Asc^-) in the phosphate–borate buffer was sonicated for 5 min with a probe-type sonicator to obtain a clear solution of the single-walled vesicle. The sonicated solutions containing SP and Asc^- separately were cooled to 0 °C and then mixed together to provide a sample for the measurements; a 50-μL sample was transferred to an ESR cell.

In experiments to detect the flip–flop behavior of amphiphile molecules, the leakage of SP from the inner aqueous compartment of the vesicle, and the permeation of Asc^- into the vesicle, the respective sample solutions were prepared in a manner similar to that stated above (see text). The initial concentrations of various chemical species used for the respective measurements are summarized in Table II.

Table III. Structures of Molecular Assemblies[a]

amphiphile	A (dispersion)	B (sonicated)[b]
$N^+C_5Ala2C_8$	cylindrical micelle[c]	cylindrical micelle[c] (Figure 1A)
$N^+C_5Ala2C_{10}$	segmented bent lamella	segmented bent lamella
$N^+C_5Ala2C_{12}$	vesicle (bent lamella)	s vesicle
$N^+C_5Ala2C_{14}$	vesicle (Figure 1B), bent lamella (Figure 1C)	s vesicle
$N^+C_5Ala2C_{16}$	vesicle, bent lamella	s vesicle (Figure 1E), s particle
$N^+C_5Ala2C_{18}$	straight lamella	s particle (Figure 1F)
$N^+C_2Ala2C_{16}$	bent lamella, straight lamella	s vesicle, s particle
$N^+C_7Ala2C_{16}$	straight lamella	s particle
$N^+C_{10}Ala2C_{16}$	straight lamella (Figure 1D)	s particle

[a] Amphiphile concentrations were set at 5 mM unless otherwise stated. Structure given in parentheses was partly observed. Abbreviations: vesicle, multilayered vesicle; lamella, multilayered lamella; s vesicle, single-walled vesicle; s particle, small particle. [b] Sonicated with a probe-type sonicator for 2 min at a 30-W power level. [c] Amphiphile concentration: 20 mM.

Results and Discussion

Morphology of Aggregates. The aggregate morphology of the present peptide amphiphiles in aqueous media was directly observed by electron microscopy and the results are summarized in Table III. All the amphiphiles were dispersed in water at their concentrations of 5 mM with occasional shaking to provide turbid samples. Multiwalled vesicles (Figure 1B) and/or multilayered lamellae (Figure 1C) were clearly observed in electron micrographs of aqueous dispersions of the peptide amphiphiles in which the number of carbon atoms in the double-chain portion is equal to or greater than 12. On the other hand, $N^+C_5Ala2C_8$ yielded cylindrical micelles (Figure 1A) when dispersed in water at the concentration of 20 mM (no turbidity), in a manner as observed for the micellar solutions of peptide surfactants.[12] Segmented

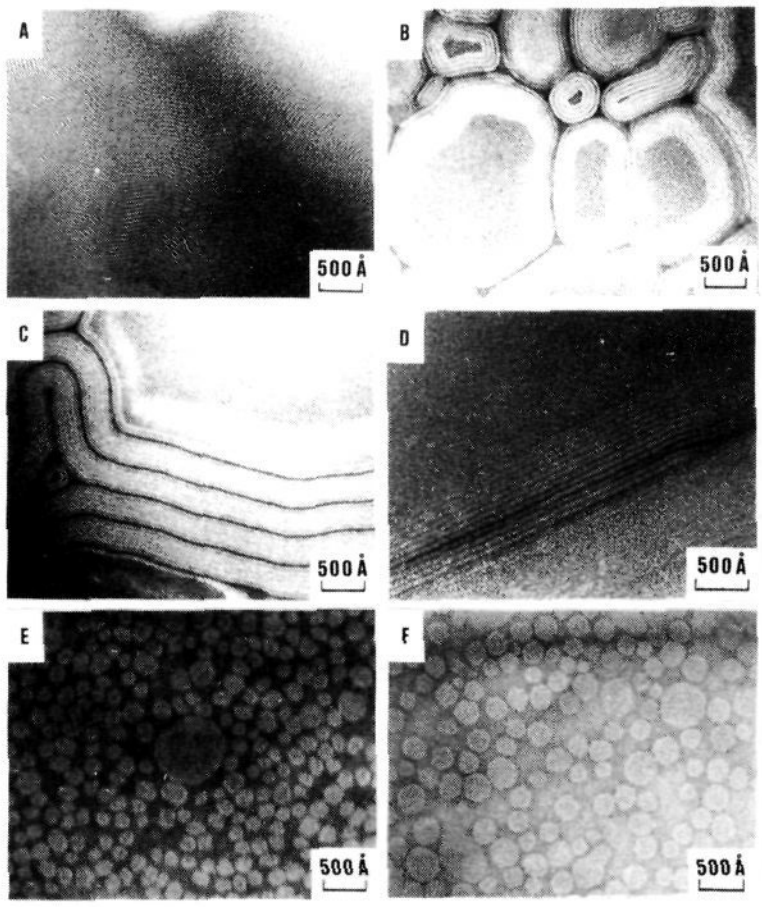

Figure 1. Electron micrographs negatively stained with uranyl acetate: A, cylindrical micelles (20 mM aqueous solution of $N^+C_5Ala2C_8$); B, multiwalled vesicles (5 mM aqueous dispersion of $N^+C_5Ala2C_{14}$); C, bent lamellae (5 mM aqueous dispersion of $N^+C_5Ala2C_{14}$); D, straight lamellae (5 mM aqueous dispersion of $N^+C_{10}Ala2C_{16}$); E, single-walled vesicles (5 mM aqueous solution of $N^+C_5Ala2C_{16}$); F, small particles (5 mM aqueous solution of $N^+C_5Ala2C_{18}$).

bent lamellae were observed in an aqueous dispersion of $N^+C_5Ala2C_{10}$. Thus, this amphiphile is regarded to be in a critical structural range for the formation of bilayer assembly. In a series of $N^+C_5Ala2C_n$ amphiphiles, the alkyl chain of the double-chain portion must be equal to or longer than the decyl group ($n \geq 10$) to form bilayer aggregates as also confirmed by differential scanning calorimetry (vide infra). Among the amphiphiles forming bilayers in the dispersion state, $N^+C_5Ala2C_{12}$ and $N^+C_5Ala2C_{14}$ compose primarily multiwalled vesicles while $N^+C_5Ala2C_{16}$ forms both multilayered vesicles and bent lamellae. However, the rest of the amphiphiles in Table III form exclusively multilayered lamellae. In particular, $N^+C_mAla2C_n$ amphiphiles, having longer molecular skeletons ($n + m \geq 23$), yield multilayered *straight* lamellae when dispersed in water (Figure 1D). If multilayered vesicles or bent lamellae were formed with an amphiphile having a longer molecular skeleton, the molecular arrangement in the bent domain would become comparatively loose due to the curvature effect (Figure 2). This may weaken hydrophobic and hydrogen-bonding interactions between the amphiphile molecules in such domains. At the extremity of the bent molecular arrangement, such thermodynamic disadvantages are relaxed by forming *straight* lamellae of bilayer aggregates. Similar structural variations of bilayer aggregates caused by the change in alkyl-chain length have been observed with cationic and anionic dialkyl amphiphiles.[13]

Sonication of aqueous dispersions with a probe-type sonicator for 2 min at a 30-W power level gave clear solutions, and the electron micrographs showed the presence of small particles with exception of the two amphiphiles: both $N^+C_5Ala2C_8$ and $N^+C_5Ala2C_{10}$ did not undergo any significant change in aggregate morphology upon sonication (Table III). Small particles observed for $N^+C_5Ala2C_{12}$ and $N^+C_5Ala2C_{14}$ (Figure 1E) are apparently single-walled vesicles having the internal aqueous compartment.

(12) Murakami, Y.; Nakano, A.; Iwamoto, K.; Yoshimatsu, A. *J. Chem. Soc., Perkin Trans. 2* **1980**, 1809–1814.

(13) Multilayered vesicles and lamellae were observed for both aqueous dispersions and sonicated solutions: (a) Kunitake, T. *J. Macromol. Sci., Chem.* **1979**, *A13*, 587–602. (b) Kunitake, T.; Okahata, Y. *Bull. Chem. Soc. Jpn.* **1978**, *51*, 1877–1879.

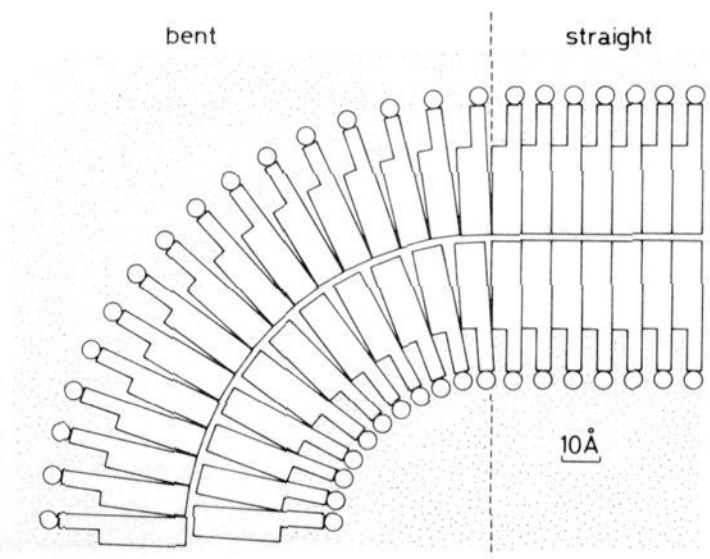

Figure 2. Two-dimensional representation of molecular arrangement in bent and straight lamellae domains in bilayer aggregates of $N^+C_5Ala2C_{18}$; open circles represent the ammonium head groups.

Table IV. Phase Transition Parameters for Peptide Amphiphiles in Aqueous Dispersion

amphiphile	concentration, w/w %	T_m, °C	ΔH, kcal/mol
$N^+C_5Ala2C_8$	2.1		
$N^+C_5Ala2C_{10}$	2.4	−44.0	0.3
$N^+C_5Ala2C_{12}$	2.3	−24.0	2.6
$N^+C_5Ala2C_{14}$	1.8	2.0	4.9
$N^+C_5Ala2C_{16}$	2.1	25.5	7.8
$N^+C_5Ala2C_{18}$	1.7	41.0	9.9
$N^+C_2Ala2C_{16}$	1.5	25.5	7.9
$N^+C_7Ala2C_{16}$	1.9	24.5	7.4
$N^+C_{10}Ala2C_{16}$	2.0	23.5	7.7

On the other hand, sonicated aqueous solutions of $N^+C_mAla2C_n$ with $n \geq 16$ involve small particles without the internal aqueous compartment (Figure 1F), although such particles were transformed into single-walled vesicles under stronger sonication conditions. However, the internal aqueous compartment was not so clearly seen for the single-walled vesicles formed with $N^+C_mAla2C_n$ ($n \geq 16$) as for those with $N^+C_5Ala2C_n$ ($n = 12$ and 14). The longer the alkyl-chain length of double-chain portion, the stronger the sonication conditions are required for the formation of single-walled vesicles.

Differential Scanning Calorimetry. The phase transition parameters (enthalpy change, ΔH; temperature at peak maximum, T_m) of the bilayer aggregates were directly measured by differential scanning calorimetry (DSC) as summarized in Table IV. Aqueous dispersions of the amphiphiles were used for the measurements unless otherwise stated. A good linear correlation between T_m and the alkyl-chain length of double-chain portion was observed for a series of $N^+C_5Ala2C_n$: 20 °C change per two methylene groups. On the other hand, the $N^+C_mAla2C_{16}$ amphiphiles show nearly identical T_m values irrespective of C_m. This finding necessitates the definition of the effective alkyl-chain length for correlation of T_m with hydrophobicity of the double-chain segment. The $N^+C_5Ala2C_n$ amphiphiles have two alkyl chains substituted on the same amide nitrogen so that the flexibility of the first three methylene groups bonded to the amide nitrogen in the double-chain segment is much restricted as confirmed by their CPK molecular models. Consequently, the T_m value is primarily controlled by the hydrophobicity of the double-chain segment, which is subjected to change by the number of the methylene groups that can rotate around the C–C bond without much steric hindrance.

The ΔH value is also linearly correlated with the alkyl-chain length of the double-chain segment. The ΔH increment per methylene group is 1.2 kcal/mol, which is comparable to that for diacylphosphatidylcholines (PC) (1.0 kcal/mol).[3a] On the basis of this correlation, the enthalpy change for the phase transition becomes zero when the n value becomes 9 or less for $N^+C_5Ala2C_n$. This again indicates that an alkyl chain in the double-chain

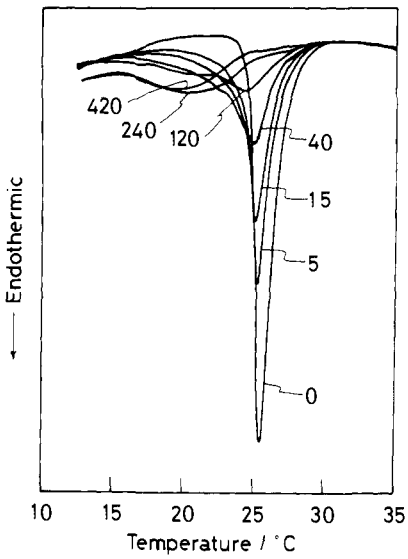

Figure 3. DSC thermograms for 1.2 w/w % aqueous dispersion of $N^+C_5Ala2C_{16}$ sonicated with a probe-type sonicator: heating rate, 2 °C/min; chart speed, 0.5 cm/min. Numerals refer to sonication time in second.

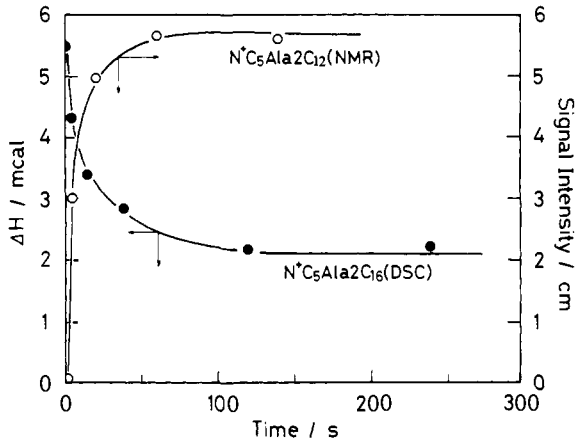

Figure 4. Correlations of ^1H NMR signal intensity for methylene resonance (in D_2O) and enthalpy change for phase transition (ΔH) with sonication time: aqueous dispersions of $N^+C_5Ala2C_n$ (n = 12, 16).

segment must be longer than the nonyl group for the amphiphiles to form bilayers.

The phase transition parameters (T_m and ΔH) change gradually as the sonication time is extended. The endothermic peak is broadened and somewhat shifted to lower temperature until multilayered aggregates are completely transformed into single-walled vesicles. One typical example of such DSC behavior for the aqueous $N^+C_5Ala2C_{16}$ system is shown in Figure 3. The ^1H NMR signal for methylene groups becomes increasingly intense as the transformation of multilayered into single-walled aggregates proceeds. Correlations of ^1H NMR signal intensity and ΔH evaluated by DSC analysis with sonication time are shown in Figure 4. Both correlation curves apparently show quite similar behavior. The T_m values obtained for the single-walled vesicles formed with amphiphiles having longer alkyl chains ($n \geq 16$) are 5–7 °C lower than those for the corresponding multilayered ones, while the ΔH values for the former are about 40% of those for the latter. The T_m and ΔH values for the amphiphiles that have shorter alkyl chains ($n \leq 14$) could not be determined accurately for their sufficiently sonicated aqueous solutions because these endothermic peaks are very weak and broad. This may be attributed to the difference in the molecular packing mode between amphiphiles having longer and shorter double chains, as suggested for PC's.[3b]

Chemical and Morphological Stability of Bilayer Aggregates. The present amphiphiles involve neither a phosphate ester nor a carboxylic ester moiety as a molecular component and therefore are expected to be chemically much more stable than PC's in aqueous media. The chemical stability of these bilayer aggregates toward acid and alkaline hydrolyses was examined by DSC. A sample of $N^+C_5Ala2C_{16}$ taken into 2 M aqueous sodium hydroxide was warmed for 5 min at 40 °C with shaking and allowed to stand at room temperature (25 ± 1 °C) with occasional shaking to obtain the aqueous dispersion for the DSC measurements. After it was allowed to stand for 3 days at room temperature, the sample solution was further heated for 4 h at 80 °C. The ΔH and T_m values did not undergo any meaningful change by these treatments. On the other hand, dimyristoyl-L-α-phosphatidylcholine (DMPC) was rapidly hydrolyzed during the initial treatment (warming for 5 min at 40 °C in aqueous 2 M NaOH) to yield white precipitates. The chemical stability of the multilayered aggregates in 2 M aqueous hydrochloric acid was examined by the similar method. Although the ΔH value for the aqueous system of DMPC decreased gradually on standing at room temperature in such an acidic medium, the value for the multiwalled aggregates of $N^+C_5Ala2C_{16}$ did not undergo meaningful change under the comparable conditions. However, the latter amphiphile was hydrolyzed gradually upon heating its aqueous dispersion at 80 °C. As shown in Figure 5, the present peptide amphiphiles as aggregated in aqueous media are much more chemically stable than PC's and other naturally occurring phospholipids.[3a]

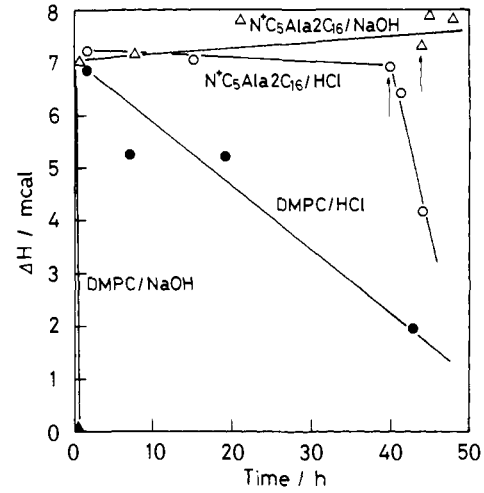

Figure 5. Time courses of heat of phase transition (ΔH) for aqueous alkaline (triangle) and acidic (circle) dispersions of $N^+C_5Ala2C_{16}$ (open) and DMPC (closed). At the points indicated by arrows, samples started to be heated at 80 °C. Concentrations: $N^+C_5Ala2C_{16}$, 1.5 w/w % in 2 M HCl and 1.6 w/w % in 2 M NaOH; DMPC, 1.4 w/w % in 2 M HCl and 1.5 w/w % in 2 M NaOH.

The sonicated solutions of the present amphiphiles, which were allowed to stand at and above their T_m's, remained clear over a month at least without any additives, and their electron micrographys retained the original patterns observed for freshly prepared solutions. This seems to indicate that the single-walled vesicles formed with $N^+C_mAla2C_n$ are structurally stable for a reasonably prolonged period of time in aqueous media. The thickness of bilayers, regardless of multi- or single-walled aggregates, ranges from 35 to 55 Å as evaluated from their electron micrographs. These values are approximately twice the length of the double-chain segments of the amphiphiles. Other supporting evidence for the high structural stability of single-walled vesicles is also provided by turbidity and NMR measurements on the sonicated aqueous solutions of $N^+C_5Ala2C_{16}$. The growth of small single-walled liposomes to larger aggregates is known to occur when the former vesicles are incubated at an appropriate temperature. The liposome-growing process was investigated by monitoring the turbidity increase of aqueous liposome solutions.[8c,14] When a vesicle solution of DMPC was incubated at temperatures even

(14) (a) Sundler, R.; Papahadjopoulos, D. *Biochim. Biophys. Acta* **1981**, *649*, 743–750. (b) Liao, M.-J.; Prestegard, J. H. *Ibid.* **1980**, *599*, 81–94.

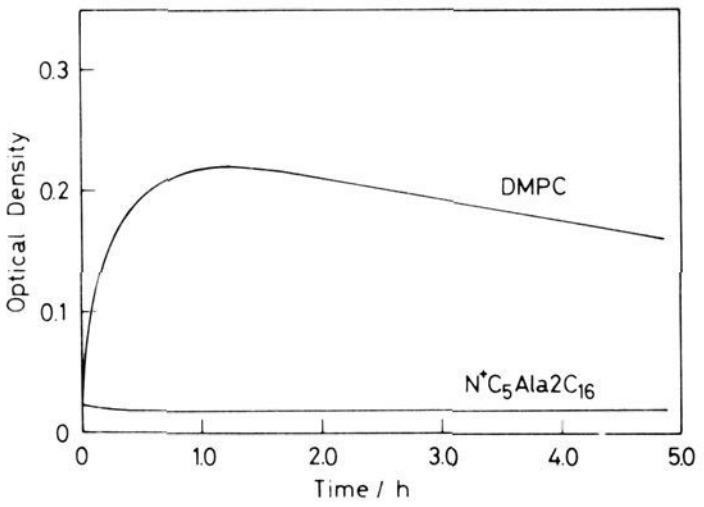

Figure 6. Time courses of turbidity change for sonicated aqueous solutions of $N^+C_5Ala2C_{16}$ (20.0 mM) and DMPC (20.0 mM) in KH_2PO_4 (69 mM)–$Na_2B_4O_7$ (15 mM) at pH 6.70, μ 0.1 (KCl), and 13.2 °C; monitored at 400 nm.

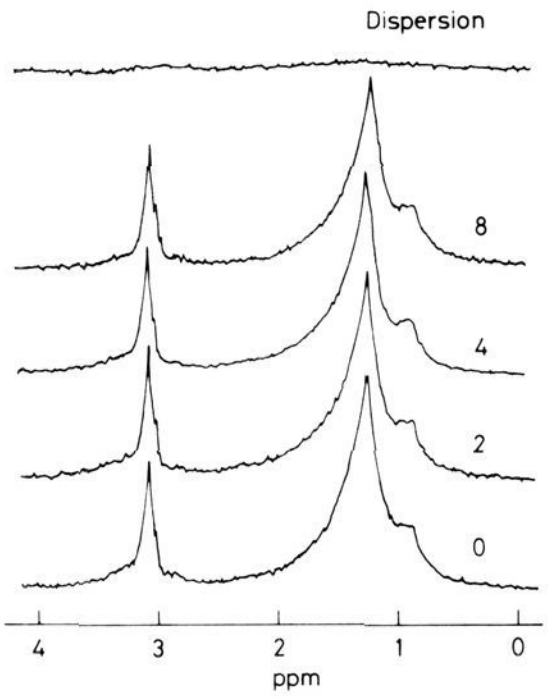

Figure 7. ^1H NMR spectral pattern for sonicated D_2O solution of 10 w/w % $N^+C_5Ala2C_{16}$ incubated at 21.0 °C; at some time intervals (in day) after preparation. The corresponding aqueous dispersion (top spectrum) involving multilayered vesicles does not show any detectable signal.

below its T_m, its turbidity increased rapidly as shown in Figure 6. On the other hand, no detectable turbidity change was observed for the sonicated aqueous solution of $N^+C_5Ala2C_{16}$ under the identical conditions. The turbidity change was not detected even when the vesicles of both $N^+C_5Ala2C_{16}$ and SP-$N^+C_5Ala2C_{16}$ (1 mL each of 10 mM solutions) were incubated together at 10.0 °C. This suggests that the net transfer, which leads to the formation of larger aggregates, does not occur under such conditions.

Similar results were also obtained by NMR studies on the sonicated aqueous (D_2O) solution of $N^+C_5Ala2C_{16}$. As the vesicle size increases, the ^1H NMR lines are broadened along with the decrease in signal intensity.[10,14b] The NMR spectrum of 10 w/w % aqueous (D_2O) solution of $N^+C_5Ala2C_{16}$ was measured at appropriate time intervals while incubated at around its phase transition temperature (21 °C). This condition was chosen because the fusion of phospholipid vesicles is drastically enhanced in their phase transition temperature range.[8b,10] No spectral change was observed during at least an 8-day period as shown in Figure 7. All the results indicate that the structures of these single-walled vesicles formed with the synthetic amphiphiles are remarkably stable as compared with those of liposomes of commercial DMPC.

Amphiphile Exchange between Single-Walled Bilayer Vesicles. The spin-labeled amphiphile, SP-$N^+C_5Ala2C_{16}$, formed multilayered lamellae in its aqueous dispersion and the aggregates were transformed completely into single-walled vesicles upon sonication for 1 min with a probe-type sonicator as shown in Figure 8. The aggregates formed with SP-$N^+C_5Ala2C_{16}$ seem to have structural characteristics such as aggregate morphology and phase transition

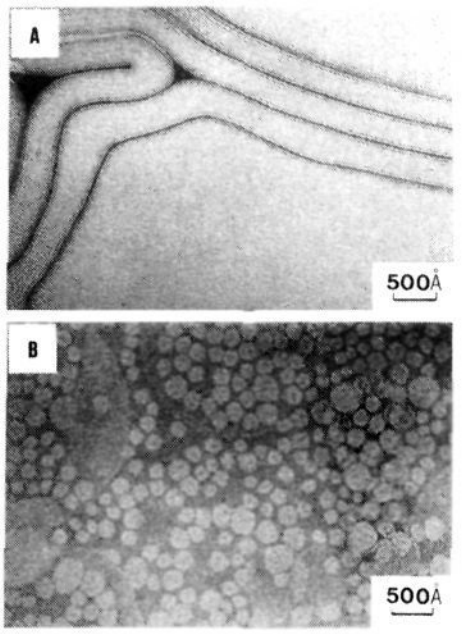

Figure 8. Electron micrographs negatively stained with uranyl acetate: A, 5 mM aqueous dispersion of SP-$N^+C_5Ala2C_{16}$; B, 5 mM aqueous solution of SP-$N^+C_5Ala2C_{16}$ sonicated for 1 min with a probe-type sonicator at 30-W power.

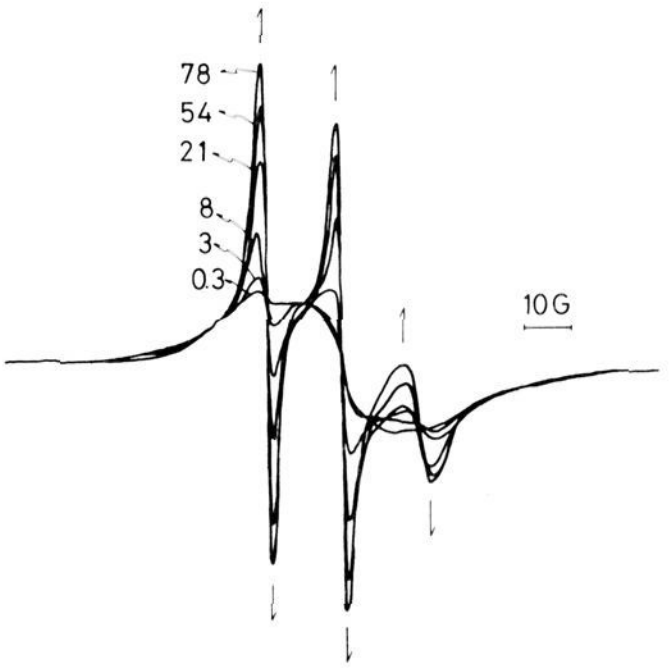

Figure 9. ESR spectral change in the course of amphiphile exchange between donor (SP-$N^+C_5Ala2C_{16}$) and acceptor ($N^+C_5Ala2C_{16}$) vesicles in KH_2PO_4 (69 mM)–$Na_2B_4O_7$ (15 mM) aqueous buffer at pH 6.70, μ 0.1 (KCl), and 35 °C: [SP-$N^+C_5Ala2C_{16}$], 0.25 mM; [$N^+C_5Ala2C_{16}$], 24.3 mM. Numerals refer to time in hour after both vesicle solutions were mixed.

parameters that are similar to those of $N^+C_5Ala2C_{16}$: for SP$N^+C_5Ala2C_{16}$, T_m = 25.6 °C and ΔH = 8.8 kcal mol^{-1}. Thus, we may reasonably conclude that both amphiphiles behave indistinguishably in their aggregated states.

All the samples used for the present investigation involve only single-walled vesicles as prepared by sonication of aqueous dispersions with a probe-type sonicator. The donor vesicles formed with SP-$N^+C_5Ala2C_{16}$ were incubated in the presence of the acceptor vesicles formed with $N^+C_5Ala2C_{16}$ in the phosphate–borate buffer at pH 6.70, μ 0.10 (KCl), and 35 °C. The amphiphile exchange was followed by ESR spectroscopy. Figure 9 shows the results obtained by using 0.25 mM SP-$N^+C_5Ala2C_{16}$ and 24.3 mM $N^+C_5Ala2C_{16}$. The time-dependent spectral change due to dilution of SP-$N^+C_5Ala2C_{16}$ with $N^+C_5Ala2C_{16}$ was clearly observed. The observed amplitude of the low-field line of the three-line spectrum (h_{dr}) for the donor vesicle homogeneously diluted with $N^+C_5Ala2C_{16}$ was plotted against the dilution parameter (r_d), $([S^*]_c + [S])/[S^*]_c$. Here, $[S^*]_c$ and [S] refer to concentrations of the labeled and unlabeled amphiphiles, respectively, and the former was set at a constant value (0.25 mM) throughout this work. The observed signal amplitude of the low-field line (h_{dr}) remained unchanged on standing overnight at a fixed temperature. Thus, the possibility of the phase separation behavior is completely excluded under present conditions. The

Table V. Kinetic Parameters for Various Dynamic Processes[a]

temp, °C	amphiphile exchange[b]		amphiphile flip–flop		permeation of Asc^-		leakage of SP		fusion assay[f]	
	k_{ex}, h^{-1}	$t_{1/2}$, h	k_{out}, h^{-1}	k_{in}, h^{-1}	$k_{perm} \times 10^6$, Mh^{-1}	$t_{1/2}$, h[c]	k_{leak}, h^{-1}	$t_{1/2}$, h	k_f, h^{-1}	$t_{1/2}$, h
10.0	0.0034	203			~0		0.03	23.1	0.029	23.9
25.0	0.0110	63	0.063	0.020	~0		0.36	1.92	0.33	2.10
35.0	0.0143	48	0.099	0.033	2.40	11.0	1.80[d] (1.93)[e]	0.38[d] (0.36)[e]	1.87	0.37

[a] See Table II for experimental conditions. [b] Concentrations: $N^+C_5Ala2C_{16}$, 24.3 mM; SP-$N^+C_5Ala2C_{16}$, 0.25 mM. [c] Half-life for disappearance of SP-$N^+C_5Ala2C_{16}$ spin probe. [d] Graphically evaluated, see text. [e] Permeation of Asc^- neglected for comparison with fusion assay. [f] Rate for disappearance of radical species (SP).

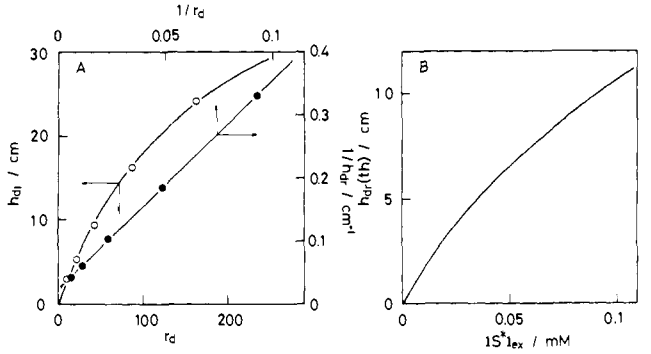

Figure 10. (A) Correlation between h_{dr} and r_d observed for homogeneously mixed vesicles of SP-$N^+C_5Ala2C_{16}$ (0.25 mM) and $N^+C_5Ala2C_{16}$ in KH_2PO_4 (69 mM)–$Na_2B_4O_7$ (15 mM) aqueous buffer at pH 6.70, μ 0.1 (KCl), and 35 °C. (B) Correlation curve for h_{dr}(th) vs. $[S^*]_{ex}$ based on eq 1 in the same medium at 35 °C; $[N^+C_5Ala2C_{16}]$, 24.3 mM.

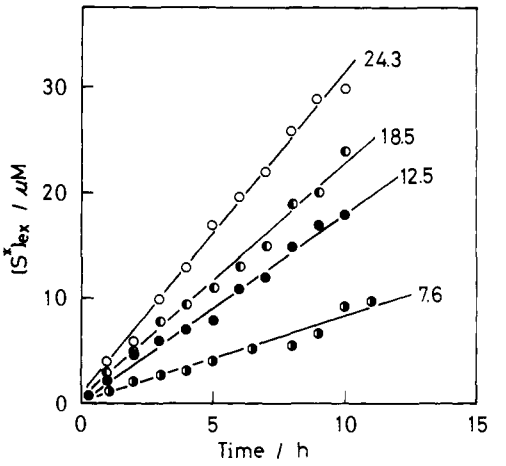

Figure 11. Time courses for amphiphile exchange between donor and acceptor vesicles in KH_2PO_4 (69 mM)–$Na_2B_4O_7$ (15 mM) aqueous buffer at pH 6.70, μ 0.1 (KCl), and 35 °C; [SP-$N^+C_5Ala2C_{16}$], 0.25 mM. Numerals indicate concentrations of $N^+C_5Ala2C_{16}$ in mM.

relationship between h_{dr} and r_d for $[S^*]_c = 0.25$ mM is shown in Figure 10A.[15] The theoretical amplitude h_{dr}(th) was calculated from eq 1 for the initial stage of the one to one exchange of the

$$h_{dr}(\text{th}) = (h^A{}_{dr}/[S^*]_c)[S^*]_{ex} + (h^D{}_{dr}/[S^*]_c)([S^*]_0 - [S^*]_{ex}) \quad (1)$$

spin-labeled amphiphile with the unlabeled one under the condition that the flip–flop time rate is much greater than the exchange time rate. Here, $h^A{}_{dr}$ and $h^D{}_{dr}$ are the calculated low-field signal amplitude caused by the labeled amphiphile molecules transferred to the acceptor vesicles and that caused by the remaining ones in the donor vesicles, respectively. These values were obtained from the correlation curve between h_{dr} and r_d (Figure 10A). $[S^*]_0$ and $[S^*]_{ex}$ are the total concentration of the labeled amphiphile and the concentration of the transferred (exchanged) one, respectively. The dilution parameters are $[S]_0/[S^*]_{ex}$ and $[S^*]_0/([S^*]_0 - [S^*]_{ex})$ for $h^A{}_{dr}$ and $h^D{}_{dr}$, respectively, under the conditions that the flip–flop time rate is much faster than the exchange time rate[16] and the gross structural features such as size and shape of the vesicles remain unchanged (see below). Here, $[S]_0$ is the total concentration of the unlabeled amphiphile used for the exchange measurements. The values of $h^A{}_{dr}/[S^*]_c$ and $h^D{}_{dr}/[S^*]_c$ on the right-hand side of eq 1 refer to the ESR amplitudes normalized to the labeled amphiphile concentration. A typical correlation curve for h_{dr}(th) vs. $[S^*]_{ex}$ is shown in Figure 10B. The amount of the transferred labeled amphiphile is evaluated from the observed ESR amplitude of the low-field line and the correlation curve established as above.

Scheme I.

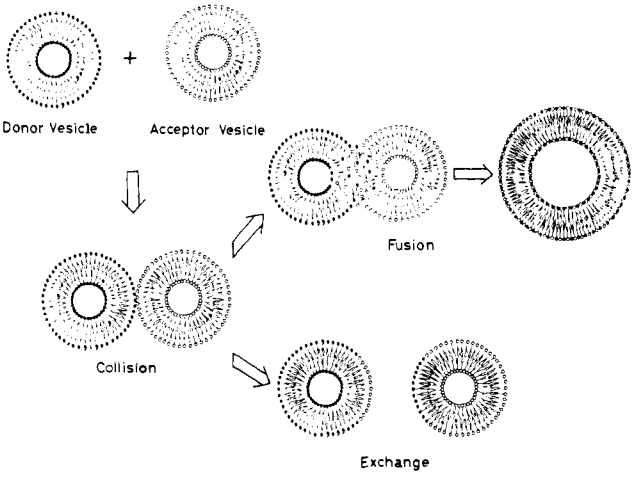

Figure 11 shows the time courses obtained for the amphiphile exchange in the presence of various amounts of the unlabeled amphiphile. Under the experimental conditions of $[S^*]_0 << [S]_0$, the exchange process follows the pseudo-first-order kinetics as given by eq 2. Here, f refers to the correction factor for the

$$\ln \frac{f[S^*]_0}{f[S^*]_0 - [S^*]_{ex}} = k_{ex}t \quad (2)$$

amount of transferable SP-$N^+C_5Ala2C_{16}$ since the overall transfer ceases at the equilibrium stage where the dilution ratios of the labeled amphiphile in both acceptor and donor vesicles become equal; $f = 1 - \{[S^*]_0/([S^*]_0 + [S]_0)\}$ (f = 0.97–0.99). A good linear relationship was obtained ($r > 0.992$) between the left-hand

(15) The correlation between h_{dr} and dilution parameter was examined at various concentrations of SP-$N^+C_5Ala2C_{16}$. The identical correlation curves for h_{dr}(th) vs. $[S^*]_{ex}$ were obtained from the corresponding h_{dr}–dilution parameter curves, regardless of the variation of the labeled-amphiphile concentration. This indicates that an amplitude of the low-field signal at a specified value of the dilution parameter is proportional to the concentration of SP-$N^+C_5Ala2C_{16}$ present in the system while the temperature is maintained constant during the measurement.

(16) If flip–flop time rate << exchange time rate, the dilution parameters are $[S]_0f_e/[S^*]_{ex}$ and $[S^*]_0f_e/([S^*]_0 - [S^*]_{ex})$ for $h^A{}_{dr}$ and $h^D{}_{dr}$, respectively, where f_e designates the fraction of the amphiphile present in the outer monolayer and can be evaluated experimentally (see text). The exchange rate constant is calculated by eq 2a in place of eq 2. The experimental data were

$$(f_ef[S^*]_0) - [S^*]_{ex} = f_ef[S^*]_0 \exp(-k_{ex}t) \quad (2a)$$

also analyzed on the basis of eq 2a, but the kinetic parameters thus obtained were in good agreement with those obtained by eq 2.

term of eq 2 and the reaction time. The pseudo-first-order rate constants obtained at several temperatures are summarized in Table V. On the basis of the results given here, we may conclude that the exchange of amphiphile molecules is a collision-mediated process between donor and acceptor vesicles rather than a diffusion-mediated one that transfers free amphiphile molecules through the bulk aqueous phase.[17-19] The second-order rate constant for the exchange process was calculated to be 5.85×10^{-4} mM^{-1} h^{-1} at 35 °C. The exchange rate obtained in this work is the slowest although it is rather difficult to make strict comparisons with others known so far because of the difference in exchange mechanism, experimental procedure, and nature of membrane system.[7,8a,c,9a,b,18d] In other words, the single-walled vesicles formed with the peptide amphiphiles are kinetically rather inert and less facile to the amphiphile exchange. The exchange process observed by the present ESR spectroscopy is consistent with the two distinct but kinetically equivalent bimolecular mechanisms shown in Scheme I: fusion of vesicles and exchange of amphiphile molecules without fusion. The fusion process for liposomal systems was detected by using several markers encapsulated into the inner aqueous compartment.[20] We prepared a hydrophilic spin probe (SP) to distinguish the above two processes and identify the real one for the present system. Before examining the fusion process, the rates of amphiphile flip–flop between the two populations of the bilayer vesicle, permeation of sodium L-ascorbate (Asc^-), and leakage of SP through the bilayer membrane were investigated.

Inside–Outside Translocation of Amphiphile Molecules in Vesicles (Flip–Flop). The time rate for the transverse movement (flip–flop) of the amphiphile molecules in single-walled vesicles was measured according to the procedure used for the phospholipid vesicles.[21] An aqueous dispersion (1 mL) of SP-$N^+C_5Ala2C_{16}$ (0.394 mM) and $N^+C_5Ala2C_{16}$ (19.8 mM) in the phosphate–borate buffer was sonicated for 1 min, and the resulting clear solution was cooled to 0 °C. A 10-μL sample of a freshly prepared aqueous solution of Asc^- (1 M) was added to the vesicle solution at 0 °C. At this stage, the paramagnetism of SP-$N^+C_5Ala2C_{16}$ located in the outer monolayer of the vesicle membrane was quenched since the vesicle is impermeable to sodium ascorbate at this temperature. This mixture was treated by gel-filtration chromatography below 5 °C (a Sephadex G-50 column of 0.8 × 32 cm, the aqueous phosphate–borate buffer as an eluant) to remove Asc^- present in the bulk aqueous phase.[22] The vesicle fraction (3.5–5.0 mL) was collected, as monitored by a UV-detector (265 nm), and 50 μL of this fraction was transferred to an ESR cell mounted on a variable-temperature probe. The asymmetry in spin-label paramagnetism of the ascorbate-treated vesicle does not persist indefinitely.[23] A signal amplitude of the low-field line increased gradually as shown in Figure 12. This must be caused by the process that the inner population of spin-labeled molecules is depleted via exchange with the outer population of nonparamagnetic molecules:

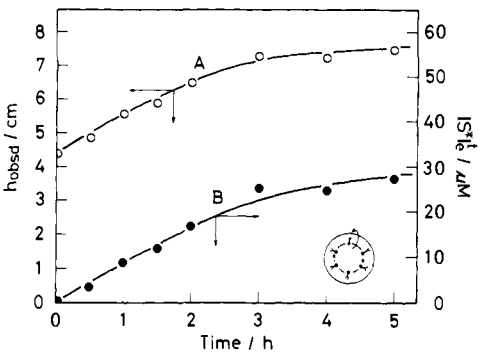

Figure 12. Time course for the flip–flop process in KH_2PO_4 (69 mM)–$Na_2B_4O_7$ (15 mM) aqueous buffer at pH 6.70, μ 0.1 (KCl), and 35 °C: A, variation of ESR signal amplitude; B, amount of translocated spin-labeled amphiphile (SP-$N^+C_5Ala2C_{16}$) from the inner layer to the outer one as evaluated from curve A in reference to eq 7.

SP-$N^+C_5Ala2C_{16}$ in inner monolayer (concentration: $[S^*]_i$)

$$k_{in} \uparrow\downarrow k_{out}$$

SP-$N^+C_5Ala2C_1$ in outer monolayer (concentration: $[S^*]_e$)

If every inward or outward translocation of paramagnetic molecules is an independent event, then the time rate of change in the internal spin-label paramagnetism is given as follows.

$$\frac{d[S^*]_i}{dt} = k_{in}[S^*]_e^t - k_{out}[S^*]_i^t \quad (3)$$

$$[S^*]_0 = [S^*]_i^t + [S^*]_e^t \quad (4)$$

Here, $[S^*]_0$ is the total concentration of SP-$N^+C_5Ala2C_{16}$ initially present in the inner monolayer of the ascorbate-treated vesicle before the flip–flop process is initiated ($t = 0$) and evaluated from the signal amplitude observed at $t = 0$ and the correlation between dilution parameter and ESR signal amplitude (see above). The superscript t indicates the value at time t. At equilibration, eq 5 holds. Here, the superscript eq designates the value at equilibrium. Combining eq 3–5 and considering also with the fact that $[S^*]_i^t + [S^*]_e^t = [S^*]_i^{eq} + [S^*]_e^{eq}$, we obtain eq 6. The

$$k_{out}[S^*]_i^{eq} = k_{in}[S^*]_e^{eq} \quad (5)$$

$$\frac{[S^*]_e^{eq}}{[S^*]_0} \ln \frac{[S^*]_e^{eq}}{[S^*]_e^{eq} - [S^*]_e^t} = k_{out}t \quad (6)$$

equilibrium of paramagnetism between the inner and outer populations of the labeled amphiphile leads to the correlation $[S^*]_e^{eq} = f_e[S^*]_0$, where f_e denotes the distributing fraction of SP-$N^+C_5Ala2C_{16}$ in the outer monolayer at equilibrium. Under conditions that the gross structural feature of vesicles remains practically unchanged during the experiments, the equilibrium distribution of paramagnetic molecules in an ascorbate-treated vesicle is identical with that in an untreated vesicle. Thus, f_e is evaluated from the signal amplitude observed for the vesicle solutions before and after the treatment with Asc^- for individual measurements. About 25% of the labeled amphiphile remained in the inner layer region. The value of $[S^*]_e^t$ was determined from the observed signal amplitude and the $h^f_{dr}(th)$ vs. $[S^*]_e^t$ correlation curve (see Figure 10). The theoretical signal amplitude, $h^f_{dr}(th)$, at time t is calculated by eq 7. Here, h_{in} and h_{out} are the calculated

$$h^f_{dr}(th) = \frac{h_{in}}{[S^*]_c}([S^*]_0 - [S^*]_e^t) + \frac{h_{out}}{[S^*]_c}[S^*]_e^t \quad (7)$$

low-field signal amplitudes caused by the labeled amphiphile located in the inner and outer monolayers, respectively, at time t. The values of h_{in} and h_{out} were determined from the respective dilution parameters defined by $([S^*]_0 + [S]_0)(1 - f_e)/([S^*]_0 - [S^*]_e^t)$ and $([S^*]_0 + [S]_0)f_e/[S^*]_e^t$ on the basis of the correlation

(17) McLean, L. R.; Phillips, M. C. *Biochemistry* **1981**, *20*, 2893–2900.
(18) Thilo, L. *Biochim. Biphys. Acta* **1977**, *469*, 326–334.
(19) (a) De Kruijff, B.; Van Zoelen, E. J. J. *Biochim. Biophys. Acta* **1978**, *511*, 105–115. (b) Rothman, J. E.; Dawidowicz, E. A. *Biochemistry* **1975**, *14*, 2809–2816. (c) Shaw, J. M.; Thompson, T. E. *Ibid.* **1982**, *21*, 920–927. (d) Galla, H.-J.; Theilen, U.; Hartmann, W. *Chem. Phys. Lipids* **1979**, *23*, 239–251.
(20) (a) McConnell, H. M. In "Spin Labeling"; Berliner, L. T., Ed.; Academic Press: New York, 1976; Chapter 13. (b) Wilschut, J.; Düzgünes, N.; Fraley, R.; Papahadjopoulos, D. *Biochemistry* **1980**, *19*, 6011–6021.
(21) Kornberg, R. D.; McConnell, H. M. *Biochemistry* **1971**, *10*, 1111–1120.
(22) Anionic species such as the ascorbate ion are bound appreciably to the charged surface of cationic vesicles: Lim, Y. Y.; Fendler, J. H. *J. Am. Chem. Soc.* **1979**, *101*, 4023–4029. In this work, therefore, the ionic strength of aqueous media was maintained at 0.10 with potassium chloride so as to minimize the attachment of Asc^- on the cationic surface of vesicles. Sodium ascorbate present in the bulk aqueous phase and on the outer vesicular surface is removed by gel-filtration chromatography.
(23) The autoxidation of the reduced SP-$N^+C_5Ala2C_{16}$ species can be neglected under the present experimental conditions on the basis of the following experiment. An aqueous dispersion (1 mL) of SP-$N^+C_5Ala2C_{16}$ (0.394 mM) and $N^+C_5Ala2C_{16}$ (19.8 mM) in the phosphate–borate buffer was sonicated for 1 min with a probe-type sonicator to obtain a clear vesicle solution. Then, 0.1 mL of Asc^- (3.90 mM) was added to the vesicle solution, and the mixture was sonicated for 10 min with a bath-type sonicator. The ESR signal almost completely disappeared and was not observed to increase within the period of 4 h at 35 °C.

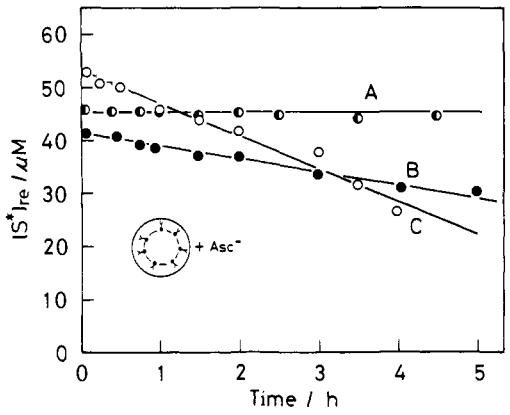

Figure 13. Time courses for permeation of sodium L-ascorbate into vesicles; in KH_2PO_4 (69 mM)–$Na_2B_4O_7$ (15 mM) aqueous buffer at pH 6.70 and μ 0.1 (KCl); $[S^*]_{re}$, amount of the remaining spin probe in the inner monolayer, at temperatures 10.0 (A), 25.0 (B), and 35.0 °C (C).

shown in Figure 10A. In this particular case, $[S]_0$ includes concentrations of both $N^+C_5Ala2C_{16}$ and SP-$N^+C_5Ala2C_{16}$ quenched with sodium L-ascorbate. In the light of the correlation curve thus obtained and an observed signal amplitude, the amount of SP-$N^+C_5Ala2C_{16}$ located in the outer layer of the vesicle at time t was evaluated and plotted as shown in Figure 12. A good linear relationship was obtained by plotting the left-hand side of eq 6 against time t ($r > 0.994$). The values of k_{in} and k_{out} thus obtained are summarized in Table V. These values at 35 °C are comparable to those for egg phosphatidylcholine[21] though they are much larger than other values for phospholipid vesicles.[24] Below T_m, no change in ESR signal was detected for a period of 5 h, indicating that the flip–flop process is practically inhibited in such a temperature range.

Permeability of Sodium Ascorbate. A 2-mL sample of an aqueous dispersion of $N^+C_5Ala2C_{16}$ (10.0 mM) and SP-$N^+C_5Ala2C_{16}$ (0.196 mM) in the phosphate–borate buffer (pH 6.70, μ 0.10 with KCl) was sonicated with a probe-type sonicator for 1 min at 30 W. Then, the sonicated solution was cooled to 0 °C, followed by addition of 40 μL of 2.5 M aqueous sodium ascorbate. At this stage, the external population of SP-$N^+C_5Ala2C_{16}$ in the mixed vesicle was immediately and completely quenched since excess sodium ascorbate reduced the nitroxide radicals immediately even at 0 °C.[21] The change of the ESR amplitude for the low-field line was monitored, and the amount of the remaining nitroxide radical was evaluated by referring to the correlation curve for ESR amplitude vs. spin-probe concentration, which was obtained by a procedure similar to that applied to the exchange experiments.[25] The amount of the remaining nitroxide radical was plotted against time as shown in Figure 13. The spin-labeled amphiphile initially located in the inner monolayer was reduced with ascorbate by way of inward permeation of the reductant and outward transverse movement of the labeled amphiphile. The rate for the permeation of Asc^- under conditions of $[SP\text{-}N^+C_5Ala2C_{16}] << [Asc^-]$ is given by eq 8, where the subscripts perm and ff denote quantities due to

$$\frac{d[Asc^-]_{perm}}{dt} = -\left(\frac{d[S^*]_{re}}{dt} + \frac{d[S^*]_{ff}}{dt}\right) = k'_{perm}[Asc^-] \cong k_{perm} \quad (8)$$

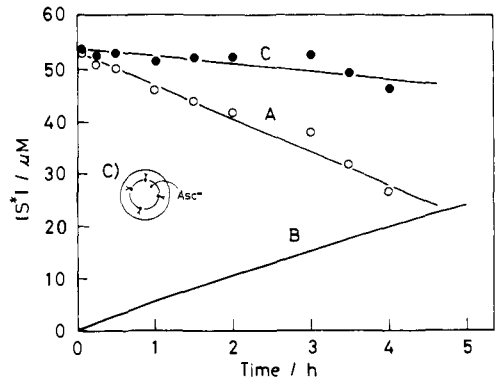

Figure 14. Time courses for the remaining spin-labeled amphiphile in the inner monolayer (A), the translocated one by flip–flop process from the inner to the outer monolayer (B, calculated in reference to the kinetic value in Table V), and quenching of the spin-labeled one in the inner monolayer due to net permeation of Asc^- (C) in KH_2PO_4 (69 mM)–$Na_2B_4O_7$ (15 mM) at pH 6.70, μ 0.1 (KCl), and 35 °C, with the following concentrations: $N^+C_5Ala2C_{16}$, 9.8 mM; SP-$N^+C_5Ala2C_{16}$, 0.19 mM; Asc^-, 49.0 mM.

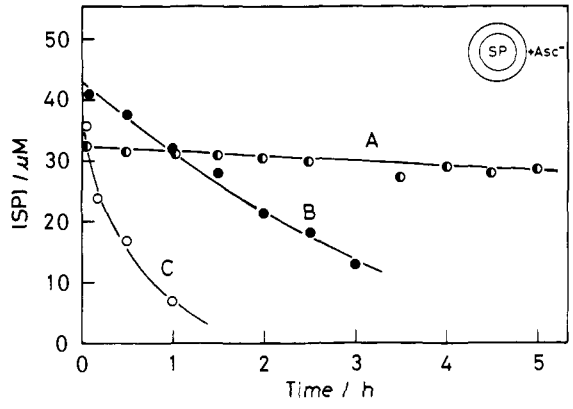

Figure 15. Time courses for quenching of SP in the internal aqueous compartment of vesicle with Asc^- in the external bulk phase; in KH_2PO_4 (69 mM)–$Na_2B_4O_7$ (15 mM) aqueous buffer at pH 6.70 and μ 0.1 (KCl), at 10.0 (A), 25.0 (B), and 35.0 °C (C). Concentrations: $N^+C_5Ala2C_{16}$, 9.8 mM; SP, 4.94 mM; Asc^-, 49.0 mM.

permeation and flip–flop, respectively, and $[S^*]_{re}$ is the concentration of the labeled amphiphile remaining in the inner monolayer. The time course for the flip–flop behavior of SP-$N^+C_5Ala2C_{16}$ molecules from the inner monolayer to the outer one is evaluated by the aid of k_{out} values obtained by the flip–flop study as typically shown in Figure 14. The time course for the permeation of Asc^- obtained graphically (Figure 14) follows the pseudo-zero-order kinetics (refer to eq 8). The result listed in Table V indicates that Asc^- penetrates into the internal aqueous compartment at temperatures above T_m even though the rate is extremely slow.

Leakage of Hydrophilic Spin Probe from Internal Water Pool. A 40-μL sample of 2.5 M aqueous sodium L-ascorbate was added at 0 °C to a sonicated clear solution (2 mL) containing 10 mM $N^+C_5Ala2C_{16}$ and 5.04 mM SP in the phosphate–borate buffer (pH 6.70, μ 0.10 with KCl). At this stage, the free radical species in the bulk aqueous phase was reduced with Asc^-, and the remaining ESR signal was attributed to SP entrapped in the internal aqueous compartment of the vesicle; a sharp triplet signal similar to that seen in an aqueous buffer solution was also observed. This means that the interaction of the cationic SP with the cationic bilayer membrane does not take place to any detectable extent as confirmed by spectroscopic means: A_N = 16.4 G and g = 2.00. Thus, the change in signal intensity is directly related to the rate of reduction of SP. The time courses for disappearance of the spin probe observed at various temperatures are shown in Figure 15. In order to obtain the net leakage rate of SP from the internal aqueous compartment, the rate for permeation of Asc^-, which has been determined in the preceding experiment, must be subtracted from the overall rate of disappearance of SP. The first-order rate

(24) Jain, M. K.; Wagner, R. C. "Introduction to Biological Membranes"; Wiley: New York, 1980; Chapter 5.

(25) In order to evaluate the theoretical signal amplitude, $h^{re}_{dr}(th)$, at time t, the following equation was adopted.

$$h^{re}_{dr}(th) = h_{re}([S^*]_{re}/[S^*]_c)$$

Here, h_{re} is the low-field signal amplitude caused by the labeled amphiphile located in the inner monolayer in the light of the correlation curve given in Figure 10A, and $[S^*]_{re}$ is its concentration remaining in the same layer. The dilution parameter, $[([S^*]_0 + [S]_0)(1 - f_e)]/[S^*]_{re}$, was used to determine h_{re}, where $[S]_0$ include concentrations of both $N^+C_5Ala2C_{16}$ and SP-$N^+C_5Ala2C_{16}$ quenched at the beginning with sodium L-ascorbate.

Table VI. Average Vesicle Parameters for Single-Walled Vesicles

parameter entity	method	$N^+C_5Ala2C_{16}$	egg lecithin[d]
outer vesicle diameter	electron microscopy	300 Å[a]	250 ± 8 Å
bilayer thickness	electron microscopy	45 ± 10 Å	46 Å
no. of amphiphile molecules/vesicle	calculated[b]	5300 ± 1000	4000
no. of amphiphile molecules on the outer surface of the vesicle	permeation, flip-flop	74 ± 3%[c]	70.5%
no. of amphiphile molecules on the inner surface of the vesicle	permeation, flip-flop	26 ± 3%[c]	29.5%
internal volume/vesicle	leakage	$(6.8 \pm 1.5) \times 10^{-18}$ cm^3	2.2×10^{-18} cm^3
inner vesicle diameter	calculated[e]	230 ± 20 Å	

[a] Outer vesicle diameter ranges from 140 to 500 Å. [b] Calculated from the weight-average molecular weight of the single-walled vesicle of $N^+C_5Ala2C_{16}$: $(4.1 \pm 1.0) \times 10^6$ g mol^{-1} by using a low-angle laser light scattering photometer LS-8 (Toyo Soda Manufacturing Co., Ltd., Tokyo, Japan); reference material, poly(ethylene oxide) (Toyo Soda RE-4, 14.8×10^4 g mol^{-1}). [c] Average value based on both permeation and flip-flop measurements. [d] Taken from literature: Hauser, H.; Oldani, D.; Phillips, M. C. *Biochemistry* **1973**, *12*, 4507-4517. [e] Calculated from the value of internal volume/vesicle estimated as follows: all the vesicles, which are involved in the phosphate-borate buffer (pH 6.70) containing 9.8 mM $N^+C_5Ala2C_{16}$, entrapped in their aqueous compartments as much as 0.65–0.85% of the total amount; the total volume of aqueous compartment being $(7.5 \pm 1.0) \times 10^{-3}$ cm^3 per mL of the vesicle solution. This value together with the aggregation number gives the listed value.

constants for the leakage of SP obtained in the T_m range and below are summarized in Table V. The half-life for the leakage of SP at 35 °C is nearly comparable to that reported for the leakage of tempocholine from the vesicle of dimyristoyl-L-α-phosphatidylcholine[26] though a rate maximum was not observed at the phase transition temperature range in the present study.

Assay on Fusion Process. In the light of the permeation and leakage behavior of charged species across the vesicular membrane as clarified in the present study, the possibility of fusion behavior of the vesicles was examined by mixing the unlabeled vesicles containing SP with those involving Asc^- in their internal aqueous compartments. Aqueous buffer solutions (1 mL each) of $N^+C_5Ala2C_{16}$ (9.8 mM) containing 4.94 mM SP and 98.0 mM Asc^- were sonicated individually for 1–2 min at 30-W power. After being cooled to 0 °C, both solutions were mixed together and an aliquot of the mixture (50 μL) was transferred to an ESR cell. When both solutions were mixed, the nitroxide radical present in the bulk aqueous phase was instantaneously and completely quenched with excess Asc^- and the ESR signal due to SP entrapped in the internal aqueous compartment was observed. The signal intensity decayed approximately exponentially as shown in Figure 16, and the observed rate data are listed in Table V. No significant disagreement between the rates of disappearance of the radical species and the corresponding rates in the leakage experiments was found at any temperatures (Figure 16). Thus, the vesicle fusion did not occur to any detectable extent within the time scale employed at every temperature. On the other hand, the exchange of amphiphile molecules was clearly seen between the donor and acceptor vesicles even at 10 °C as shown in Figure 16. Furthermore, the rate of disappearance of SP in the fusion assay was not affected by the addition of various substances such as 1.0 mM myristic acid, 1.0 mM myristylamine, 10.0 mM citric acid, and 1.9 mM cholesterol at 10 °C. The results indicate that the single-walled vesicles formed with the peptide amphiphiles are so stable that the fusion process is inhibited under ordinary conditions. Such structural stability seems to originate partly in the charge effect provided on the vesicular surface, which gives out an effective electrostatic repulsive force for the vesicle–vesicle interaction, and partly in the thermodynamic effect. The latter effect must be due to the strong hydrophobic interaction in the interior double-chain domain, assisted by the hydrogen-bonding interaction effective in the so-called hydrogen-belt domain.

In order to confirm the validity of these experiments, the fusion assay was applied to the vesicle of dimyristoyl-L-α-phosphatidylcholine of commercial source (DMPC, 98% purity). An aqueous dispersion of DMPC was sonicated under identical conditions as stated above. The time course for the disappearance of SP entrapped in the internal aqueous compartment of liposomal vesicle (refer to SP leakage experiments, curve A) and that for

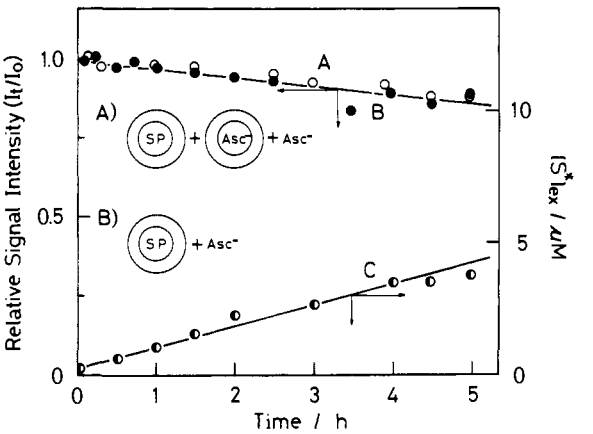

Figure 16. Time courses for decay of the ESR signal amplitude due to SP [A (○), fusion assay; B (●), SP leakage], and time course for amphiphile exchange between donor and acceptor vesicles (C) in KH_2PO_4 (69 mM)–$Na_2B_4O_7$ (15 mM) aqueous buffer at pH 6.70, μ 0.1 (KCl), and 10.0 °C. A: $[N^+C_5Ala2C_{16}]$, 9.8 mM; [SP], 4.94 mM (inside one vesicle system); $[Asc^-]$, 98.0 mM (inside another vesicle system without SP) and 46.6 mM (in bulk phase). B: $[N^+C_5Ala2C_{16}]$, 9.8 mM; [SP], 4.94 mM (inside vesicle); $[Asc^-]$, 46.6 mM (in bulk phase). C: $[N^+C_5Ala2C_{16}]$, 24.3 mM; $[SP\text{-}N^+C_5Ala2C_{16}]$, 0.25 mM.

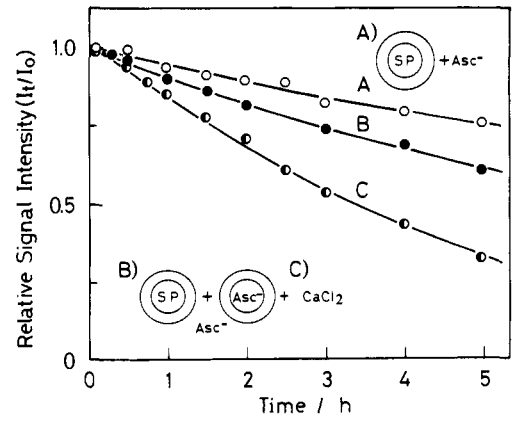

Figure 17. Time courses for decay of the ESR signal amplitude due to SP entrapped in the internal aqueous compartment of DMPC liposome in KH_2PO_4 (69 mM)–$Na_2B_4O_7$ (15 mM) at pH 6.70, μ 0.1 (KCl), and 10 °C: A, SP leakage; B, fusion assay without $CaCl_2$; C, fusion assay with $CaCl_2$. A: [DMPC], 9.8 mM; [SP], 4.94 mM; $[Asc^-]$, 49.0 mM in bulk phase. B: [DMPC], 9.8 mM; one vesicle system containing [SP] = 4.94 mM in both vesicular and bulk phases; another system containing $[Asc^-]$ = 98.0 mM in both vesicular and bulk phases; both vesicle systems were mixed after individual preparation. C: $[CaCl_2]$ = 10.1 mM in bulk phase; in addition to the components identical with B.

(26) Marsh, D.; Watts, A.; Knowles, P. F. *Biochemistry* **1976**, *15*, 3570–3578.

the fusion assay (curve B) at 10 °C are shown in Figure 17. The results clearly indicate that the fusion process does take place with the DMPC vesicles. The process was further accelerated upon addition of calcium ions ($CaCl_2$)[8c,20] (curve C in Figure 17).

Concluding Remarks

As listed in Table VI, all the physical parameters for single-walled vesicles of $N^+C_5Ala2C_{16}$ and egg lecithin are comparable to each other. In other words, the physical shape and amphiphile aggregation mode of the vesicles of peptide amphiphiles are nearly identical with those of the vesicles of naturally occurring phospholipids having aliphatic double chains of comparable sizes. However, the single-walled vesicles formed with the former amphiphiles are structurally much more stable than those with the latter and stay in solution over at least a month without meaningful morphological change. Such structural stability seems to originate in the formation of stronger hydrogen-belt domains through intravesicular hydrogen-bonding interaction between the amino acid residues. The present amphiphiles do not undergo hydrolysis even in acidic and alkaline media at room temperature for a reasonably prolonged period of time, while diacylphosphatiylcholines are readily decomposed under the same conditions.

Even though the intervesicular exchange of the amphiphile molecules takes place between the single-walled vesicles via a collision mechanism, they do not undergo fusion to form larger aggregates in a reasonably prolonged period of time. Permeability of charged water-soluble materials across the bilayer membrane is extremely sluggish and nearly inhibited at temperatures below T_m. The present results suggest that these peptide amphiphiles have great potential to become effective drug carriers in the state of single-walled vesicles.

Acknowledgment. The present work was supported in part by a Grant-in-Aid for Scientific Research from the Ministry of Education, Science and Culture of Japan (No. 58430016).

Registry No. DMPC, 18194-24-6; SP, 89637-61-6; SP-$N^+C_5Ala2C_{16}$, 89637-60-5; $N^+C_5Ala2C_8$, 89637-54-7; $N^+C_5Ala2C_{10}$, 89637-55-8; $N^+C_5Ala2C_{12}$, 78761-16-7; $N^+C_5Ala2C_{14}$, 83825-02-9; $N^+C_5Ala2C_{16}$, 88598-40-7; $N^+C_5Ala2C_{18}$, 89637-56-9; $N^+C_2Ala2C_{16}$, 89637-57-0; $N^+C_7Ala2C_{16}$, 89637-58-1; $N^+C_{10}Ala2C_{16}$, 89637-59-2; $2C_1NC_5Ala2C_{16}$, 89637-62-7; *N*-(1-oxyl-2,2,6,6-tetramethyl-4-piperidyl)iodoacetamide, 25713-24-0; ascorbic acid, 50-81-7.

Quantum Mechanical and Molecular Mechanical Studies on a Model for the Dihydroxyacetone Phosphate–Glyceraldehyde Phosphate Isomerization Catalyzed by Triosephosphate Isomerase (TIM)

Giuliano Alagona,† Peter Desmeules, Caterina Ghio,† and Peter A. Kollman*

Contribution from the Department of Pharmaceutical Chemistry, School of Pharmacy, University of California, San Francisco, California 94143. *Received July 13, 1983*

Abstract: We have carried out ab initio (SCF + MP2) and molecular mechanical calculations on a model for the reaction catalyzed by triosephosphate isomerase. To our knowledge, this is the first time that ab initio SCF, correlation energy, and environmental effect calculations have been carried out on all the chemical steps of an enzymatic reaction, along with molecular mechanical simulation of some steps. The quantum mechanical calculations show how the TIM-catalyzed reaction, one of the most efficient known, can have as its rate-limiting step product dissociation in that the effect of the enzyme is to make the *chemical* steps very rapid. The enzyme does this by stabilizing the enzyme–intermediate complex so that it becomes of approximately equal stability to the enzyme–substrate complex. This lowers the barrier between these species to the range of 10–15 kcal/mol. The molecular mechanical calculations have been used to generate refined coordinates for the enzyme–substrate and enzyme–intermediate complexes, which were essential in evaluating environmental effects on the quantum mechanical energies. They have also been used to suggest the effect of genetic mutation of the key active site histidine residue in TIM to a glutamine. Our calculations suggest the chemical steps in this mutant TIM will be less effective than in the normal enzyme, for reasons which had not been suggested heretofore.

One of the most efficient enzyme-catalyzed reactions is the triosephosphate isomerase (TIM) catalyzed reversible isomerization of dihydroxyacetone phosphate (DHAP) to glyceraldehyde 3-phosphate (GAP). In an elegant set of papers, using isotope labeling and kinetic methods, Knowles and co-workers[1] determined a complete free energy profile for the enzyme-catalyzed reaction and suggested that this enzyme was "perfectly evolved" in that the rate-determining step for the DHAP ⇌ GAP isomerization was product dissociation from the enzyme. Thus, there is no evolutionary pressure for the enzyme to improve the catalytic efficiency of the reactive steps on the enzyme. The enzyme-catalyzed reaction of TIM should be a very interesting one to study in that it should give us insight into how the enzyme achieves its enormous catalytic rate enhancement (10^9 over the uncatalyzed reaction). The mechanism of the TIM-catalyzed reaction is reasonably well understood (Schemes I and II).

Scheme I

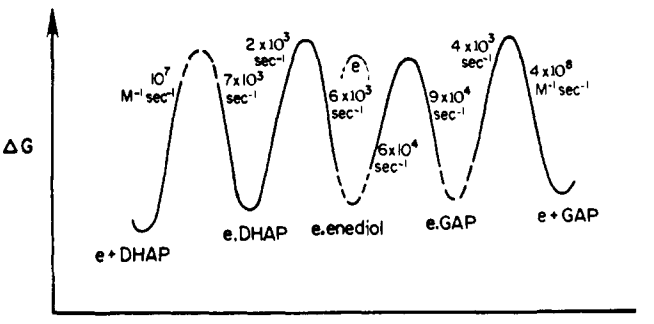

Scheme I details the free energy profile suggested by Knowles et al.,[1] in which there are five species: e + DHAP (separated enzyme + dihydroxyacetone phosphate), e·DHAP (Michaelis

† Permanent address: Istituto di Chimica Quantistica ed Energetica Molecolare del C.N.R., Pisa, Italy.

(1) Leadlay, P. F.; Albery, W. J.; Knowles, J. R. *Biochemistry* **1976**, *15*, 5617. Albery, W. J.; Knowles, J. R. *Ibid.* **1976**, *15*, 5588, 5627.

0002-7863/84/1506-3623$01.50/0